JACS
JOURNAL OF THE AMERICAN CHEMICAL SOCIETY
Article
pubs.acs.org/JACS

A Complete Family of Terminal Uranium Chalcogenides, $[U(E)(N\{SiMe_3\}_2)_3]^-$ (E = O, S, Se, Te)

Jessie L. Brown, Skye Fortier, Richard A. Lewis, Guang Wu, and Trevor W. Hayton*

Department of Chemistry and Biochemistry, University of California, Santa Barbara, California 93106, United States

Supporting Information

ABSTRACT: Addition of 1 equiv of E (E = 0.125 S_8, Se, Te) to $U(H_2C{=}PPh_3)(NR_2)_3$ (R = $SiMe_3$) (**1**) in Et_2O results in generation of the terminal chalcogenide complexes, $[Ph_3PCH_3][U(E)(NR_2)_3]$ (E = S, **2**; Se, **3**; Te, **4**; R = $SiMe_3$), in modest yield. Complexes **2**–**4** represent extremely rare examples of terminal uranium monochalcogenides. Synthesis of the oxo analogue, $[Cp^*_2Co][U(O)(NR_2)_3]$ (**5**), was achieved by reduction of $[U(O)(NR_2)_3]$ with Cp^*_2Co. All complexes were fully characterized, including analysis by X-ray crystallography. In the solid state, complexes **2**–**5** feature short U–E bond lengths, suggestive of actinide–ligand multiple bonding.

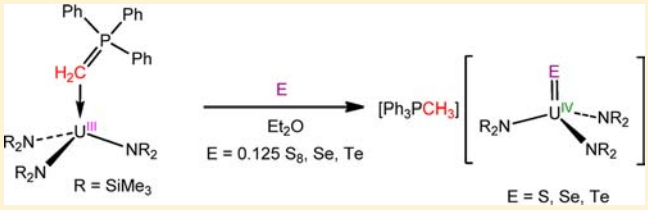

INTRODUCTION

The separation of late actinides, Am and Cm, from the lanthanide fission products in spent nuclear fuel would greatly facilitate its long-term storage.[1−3] The most promising ligands for effecting this separation are those containing soft donors (e.g., N, S), an observation that has been rationalized on the basis of increased covalency within An–L bonds versus Ln–L bonds.[4−7] In an effort to improve the performance of soft donor ligands, there has been an increased effort to synthesize new complexes containing actinide–soft donor interactions, with the goal of understanding the electronic structure of the resulting An–L bonds.[4,5,8] While this work has expanded our knowledge base, actinide complexes containing An–S, and especially An–Se and An–Te interactions, are still relatively rare.[9]

To address this paucity of knowledge, we have endeavored to synthesize complexes that contain U–E (E = S, Se, Te) bonds, specifically those containing the terminal monochalcogenido functionality, as this ligand type is exceptionally rare for the actinides. Previous attempts to generate terminal monosulfido, -selenido, and -tellurido complexes of the actinides have yielded bridging chalcogenide ligands.[10−16] For example, Meyer and co-workers isolated a series of uranium chalcogenide complexes exhibiting bridging E^{2-} ligands, $[((^{tBu}ArO)_3tacn)U]_2(\mu\text{-}E)$ (E = O, S, Se) and $[Na(DME)_3]_2[(((^{Ad}ArO)_3N)U)_2(\mu\text{-}E)_2]$ (E = S, Se, Te), which were formed by chalcogen atom transfer to a U(III) precursor.[9] Likewise, Andersen reported the synthesis of $[(MeC_5H_4)_3U]_2(\mu\text{-}E)$ (E = S, Se, Te) using a similar approach.[10] These results suggest that the potent nucleophilicity of the chalcogenide ligands favors bridging interactions. This hypothesis is also supported by recent reactivity studies.[17]

In contrast to the scarcity of uranium complexes with heavier chalcogenide ligands, terminal mono-oxo complexes of uranium, especially for U(V) and U(VI), are now reasonably common.[18−21] For example, Meyer and co-workers have reported the synthesis of $[((^{tBu}ArO)_3tacn)UO]$ and $[((^{tBu}ArO)_3tacn)UO][SbF_6]$.[22,23] Also of note is $(NN'_3)U(O)$ ($NN'_3 = N(CH_2CH_2NSiMe_2{}^tBu)_3$), formed by O-atom transfer to $(NN'_3)U(CH_2{=}PPh_3)$,[24] and $Cp^*_2U(O)(NAr)$, which features a cis arrangement of its oxo and imido ligands.[25−27] Finally, Liddle and co-workers recently reported the U(VI) oxo carbene complex (BIPM)$UOCl_2$ (BIPM = $[C(PPh_2NSiMe_3)_2]^{2-}$).[28] A few terminal oxo complexes are also known for U(IV). For example, Bart and co-workers recently reported the synthesis of $Tp^*_2U{=}O$.[29] This complex is similar to $Cp'_2U{=}O$ ($Cp' = 1,2,4\text{-}{}^tBu_3C_5H_2$), which was prepared by Andersen in 2005,[30] and $Cp^*_2U{=}O(NHC)$, prepared by Evans in 2004.[19] Also recently, Andrews reported the isolation of UOF_2 in an Ar matrix at 4 K.[31]

The above-mentioned body of work suggests that terminal uranium mono-sulfide, -selenide, and -telluride complexes could also be stable. However, it is likely that the development of new synthetic procedures will be necessary before their isolation is realized. In fact, the only known uranium terminal monochalcogenide complex, $[Na(18\text{-crown-}6)][Cp^*_2U(S)(S{}^tBu)]$, was generated serendipitously by reduction of $Cp^*_2U(S{}^tBu)_2$ with Na/Hg amalgam.[32] This resulted in spontaneous C–S bond homolysis and formation of a *tert*-butyl radical.[32] Interestingly, the U=S double bond (2.477(2) Å) in $[Na(18\text{-crown-}6)][Cp^*_2U(S)(S{}^tBu)]$ is notably shorter than its U–S single bond (2.744(2) Å), suggesting the presence of multiple-bond character in the U=S interaction.

Herein, we report the synthesis and characterization of a series of terminal monochalcogenido complexes of uranium, $[Ph_3PCH_3][U(E)(NR_2)_3]$ (E = S, Se, Te; R = $SiMe_3$), formed by oxidative atom transfer to a U(III)-ylide adduct, $U(H_2C{=}PPh_3)(NR_2)_3$. Their isolation is likely facilitated by the presence

Received: June 12, 2012
Published: August 25, 2012

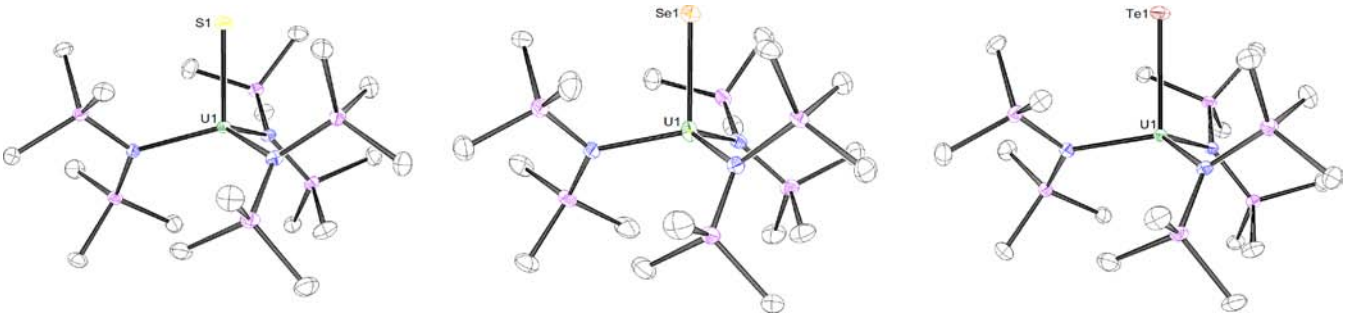

Figure 1. Solid-state molecular structures of **2** (left), **3** (middle), and **4** (right) with 50% probability ellipsoids. Hydrogen atoms and the phosphonium cation are omitted for clarity.

of the ylide ligand in the U(III) starting material, which prevents formation of a bridging chalcogenide complex by slowing the rate of comproportionation, a strategy first employed by Scott and co-workers.[18,24]

RESULTS AND DISCUSSION

Synthesis. Recently, our laboratory reported the synthesis and isolation of a U(V) terminal mono-oxo metallacycle, $[Ph_3PCH_3][U(O)(CH_2SiMe_2NSiMe_3)(NR_2)_2]$, generated by O-atom transfer from TEMPO (TEMPO = 2,2,6,6-tetramethylpiperidine-1-oxyl) to the U(III)-ylide adduct, $U(H_2C{=}PPh_3)(NR_2)_3$ (R = $SiMe_3$) (**1**).[33] This result prompted us to explore the chemistry of **1** with the other group 16 elements. Thus, addition of 0.125 equiv of S_8 to **1**, in Et_2O, results in an immediate color change from deep purple to dark orange. Crystallization of the resulting solid from THF/hexanes provides a rare U(IV) terminal monosulfido complex, $[Ph_3PCH_3][U(S)(NR_2)_3]$ (**2**), as a yellow solid in 19% yield, based on uranium (vide infra) (eq 1). Similarly, addition of 1 equiv of elemental selenium or tellurium to **1** results in the formation of $[Ph_3PCH_3][U(E)(NR_2)_3]$ (E = Se, **3**; Te, **4**), in comparable yields (eq 1). To our knowledge, complexes **3** and **4** represent the first terminal monoselenide and -telluride complexes of uranium, respectively. Interestingly, the use of $Ph_3P{=}S$ as a S-atom source did not result in formation of **2**, but only resulted in the production of an intractable reaction mixture.

Complexes **2**–**4** are thermally unstable solids; however, they can be stored for several weeks at −25 °C under an inert atmosphere without noticeable signs of decomposition. Complexes **2**–**4** are insoluble in hexanes, sparingly soluble in toluene, but quite soluble in THF, DME, and pyridine. The ^{1}H NMR spectrum of complex **2** in py-d_5 features a broad singlet at −2.24 ppm, assignable to the $SiMe_3$ groups of the silylamide ligand. Also present is a doublet at 1.43 ppm (J_{PH} = 13 Hz), assignable to the methyl group of the phosphonium counterion. The $^{31}P\{^1H\}$ NMR spectrum of **2** consists of a broad singlet at 21.3 ppm, assignable to the $[Ph_3PCH_3]^+$ moiety. The ^{1}H and ^{31}P NMR spectra of **3** and **4** are similar to those recorded for **2**.

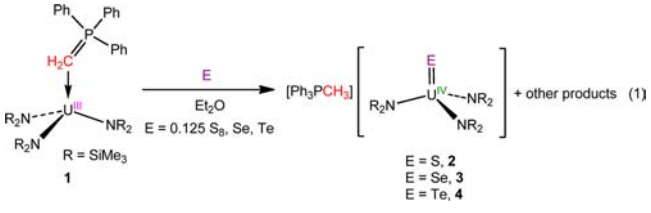

Complexes **2**–**4** crystallize in the monoclinic space group $P2_1/c$ as discrete cation/anion pairs. The solid-state molecular structures of **2**–**4** are shown in Figure 1. Tabulated metrical parameters for **2**–**4** are presented in Table 1. The uranium

Table 1. Selected Bond Distances (Å) and Angles (deg) for Complexes 2-5

	2	3	4	5
U1−E1	2.4805(5)	2.6463(7)	2.866(2)	1.878(5)
E1−C1	3.641(2)	3.718(6)	3.853(2)	
U1−N1	2.299(2)	2.280(5)	2.283(2)	2.374(5)
U1−N2	2.300(2)	2.287(5)	2.278(2)	2.362(5)
U1−N3	2.306(2)	2.286(6)	2.289(2)	2.367(5)
E1−U1−N1	104.87(4)	101.7(1)	105.46(4)	98.6(2)
E1−U1−N2	103.34(4)	99.4(1)	101.03(4)	98.0(2)
E1−U1−N3	100.24(4)	104.2(1)	99.92(4)	99.5(2)
U1···N_3 plane[a]	0.510(1)	0.464(3)	0.478(1)	0.358(3)
E covalent radius[b]	1.05	1.20	1.38	0.66

[a]Defined as the displacement of U1 out of the plane formed by the three nitrogen atoms. [b]Taken from ref 38.

center in the $[U(S)(NR_2)_3]^-$ anion features a pseudotetrahedral geometry in the solid state (S1−U1−N1 = 104.87(4)°, S1−U1−N2 = 103.34(4)°, S1−U1−N3 = 100.24(4)°). The U−S bond length in **2** (U1−S1 = 2.4805(5) Å) is statistically indistinguishable from the U−S bond distance found in the only other known uranium terminal sulfide complex, $[Na(18\text{-crown-6})][U(Cp^*)_2(S^tBu)(S)]$ (U1−S1 = 2.477(2) Å),[32,34] and is considerably shorter than a typical U−S single bond (ca. 2.74 Å).[13,32,34] For further comparison, the U−S bond length in gas-phase US_2 is calculated to be shorter at 2.38 Å,[35] while the U−S bond length in $[((^{tBu}ArO)_3tacn)U]_2(\mu\text{-}S)$ is substantially longer, at 2.592(6) Å.[9] Finally, the metrical parameters of the $[Ph_3PCH_3]^+$ cation in **2** are similar to those seen previously.[33] This moiety is formally derived from protonation of the ylide ligand found in the starting material (vide infra).

As expected, the U−Se and U−Te bond distances in complexes **3** and **4** (**3**, U1−Se1 = 2.6463(7) Å; **4**, U1−Te1 = 2.866(2) Å) are substantially longer than the U−S bond distance in **2**, consistent with the larger covalent radii of Se and Te. However, the U−Se and U−Te distances in **3** and **4** are the shortest yet reported for the actinides, in line with formal U=E multiple bond character. For comparison, the U−Se distance in $[((^{tBu}ArO)_3tacn)U]_2(\mu\text{-}Se)$ is 2.7188(4) Å, while the average U−Te distance in $[[((^{Ad}ArO)_3N)U]_2(\mu\text{-}Te)_2]^{2-}$ is 3.07 Å.[9]

Interestingly, in complex **2** there is a close contact between the sulfido ligand found in the $[U(S)(NR_2)_3]^-$ anion and the methyl group of the phosphonium cation (S1−C1 = 3.641(2)

dx.doi.org/10.1021/ja305712m | J. Am. Chem. Soc. 2012, 134, 15468−15475

Å). This interaction is also observed in complexes **3** (Se1−C1 = 3.718(6) Å) and **4** (Te1−C1 = 3.853(2) Å). Nonconventional hydrogen bonding between a C−H donor and a chalcogen has been observed previously, most notably in the solid-state molecular structures of $(Me_8taa)GeE$ (Me_8taa^{2-} = tetramethyldibenzotetraaza[14]annulene dianion; E = S, Se, Te),[36,37] and their presence is suggestive of a large partial negative charge, $E^{\delta-}$, on the chalcogenide.[37] A secondary interaction is also observed in $[Na(18\text{-crown-}6)][(Cp^*)_2U(S^tBu)(S)]$, which exhibits a S−Na distance of 3.135(4) Å.[32]

To determine if this hydrogen-bonding interaction is maintained in solution, we performed ^{1}H DOSY spectroscopy on complex **3**. In py-d_5 at 25 °C, the phosphonium cation in **3** exhibits a relative diffusion constant of 0.36 (with respect to the diffusion constant of the residual protio signal of py-d_5). In comparison, $[Ph_3PCH_3][I]$ and $[Ph_3PCH_3][PF_6]$ exhibit relative diffusion constants of 0.38 and 0.40, respectively, under the same conditions. The similarity of these values suggests that the H-bonding interaction observed in the solid state is relatively weak and is easily overwhelmed by polar solvents.

For further comparison, we synthesized the mono-oxo analogue of complexes **2**−**4** by reduction of the known pentavalent mono-oxo $U(O)(NR_2)_3$ (R = $SiMe_3$)[39] with 1 equiv of Cp^*_2Co in Et_2O. Recrystallization from THF/hexanes affords the U(IV) terminal oxo complex $[Cp^*_2Co][U(O)(NR_2)_3]$ (**5**), in 81% yield (eq 2). Its ^{1}H NMR spectrum in py-d_5 features a broad singlet at −2.13 ppm, assignable to the $SiMe_3$ groups of the silylamide ligand. Also present is a singlet at 3.40 ppm, assignable to the methyl groups of the $[Cp^*_2Co]^+$ counterion.

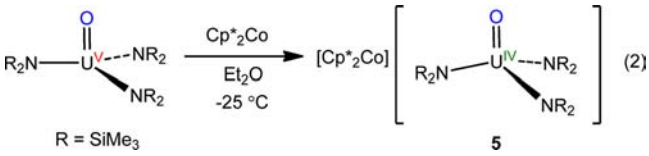

Complex **5** crystallizes in the monoclinic space group $P2_1/n$ as a discrete cation/anion pair (Figure 2). Unlike the pseudotetrahedral geometries found for complexes **2**−**4**, complex **5** is distorted toward a trigonal pyramidal geometry about the metal center (O1−U1−N1 = 98.6(2)°, O1−U1−N2 = 98.0(2)°, O1−U1−N3 = 99.5(2)°) (Table 1). A similar distortion is also seen in its U(V) parent, $U(O)(NR_2)_3$.[39] The U−O bond distance in **5** (U1−O1 = 1.878(5) Å) is slightly longer than that observed in $U(O)(NR_2)_3$ (U1−O1 = 1.817(5) Å),[39] but is comparable to other known U(IV) terminal mono-oxo complexes.[19,29,30] Also of note, the average U−N bond length in **5** is approximately 0.06 Å longer than those seen in **2**−**4**. This lengthening may result from competition between the more strongly donating dianionic oxo ligand and the less-donating monoanionic amide ligands for metal-based orbitals.

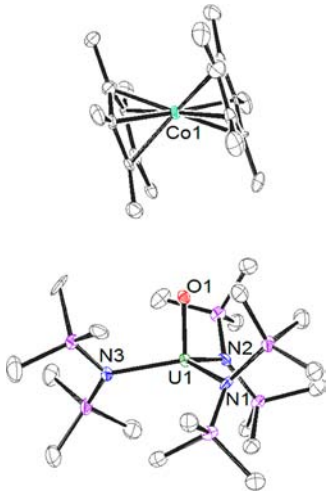

Figure 2. Solid-state molecular structure of $[Cp^*_2Co][U(O)(NR_2)_3]$ (**5**) with 50% probability ellipsoids. Hydrogen atoms are omitted for clarity.

Magnetism and Electronic Absorption Spectra. To verify the 4+ oxidation state of the uranium centers in complexes **2**−**5**, we further characterized these materials by solution-phase NIR spectroscopy and SQUID magnetometry. The NIR spectra for complexes **2**−**5** are all qualitatively similar and are comparable to the spectra seen for other U(IV) amides, including $U(I)(NR_2)_3$ and $[(R_2N)_3U]_2(\mu\text{-}O)$ (R = $SiMe_3$),[39,40] suggesting that the U(IV) oxidation state assignment is appropriate. At 300 K, complex **3** exhibits an effective magnetic moment of 3.23 μ_B, which drops precipitously to 0.96 μ_B upon cooling to 4 K (C = 1.82 emu K mol^{-1}, θ = −59 K). This behavior is also consistent with the U(IV) oxidation state assignment (Figure 3).[41−47] Similarly, complex **4** exhibits an effective magnetic moment of 2.83 μ_B at 300 K, which decreases to 0.79 μ_B at 4 K (C = 2.05 emu K mol^{-1}, θ = −98 K). While the room temperature moment for **4** is lower than the 3.58 μ_B anticipated for a $^3H_4$ ground state, the temperature dependence of the moment is typical of U(IV) complexes. In contrast to the magnetism seen for **3** and **4**, complex **5** exhibits an effective magnetic moment of 2.73 μ_B at 300 K, which only decreases slightly to 2.00 μ_B at 4 K. This different behavior may be due to the change in displacement of the uranium atom from the plane formed by the three amide nitrogens, as geometry has been previously observed to play a large role in the magnetic behavior of U(IV) complexes, especially in complexes with strong field ligands.[48] We did not perform a magnetization experiment for complex **2** because of the presence of a persistent impurity in samples of this complex (see Figure S4). This impurity has proven incredibly difficult to remove. However, it is not present in large quantities, as indicated by the acceptable elemental analysis recorded for **2**. Nonetheless, because of the incredible sensitivity of SQUID magnetometry, it is likely that its presence would affect the magnetization measurement.

We have also characterized complexes **2**−**5** via vibrational spectroscopy. For complex **2** we expect the U−S stretch to appear between 340 and 460 cm^{-1}, based on the work of the Andrews group.[35,49] However, we do not observe a stretch in this region that could be reasonably assigned to a U−S vibration. Unfortunately, the ν(U−E) stretches of **3**−**5** could not be definitively identified either. Additionally, attempts to record the Raman spectra for complexes **2**−**5** were unsuccessful due to the burning of the sample by the laser.

Mechanistic Studies. The isolation of complexes **2**−**4** raises several interesting mechanistic questions, such as the origin of the proton incorporated in the phosphonium cation. Given that the uranium centers in **2**−**4** are in the 4+ oxidation state, and that elemental chalcogens formally act as 2e$^-$ oxidants, we postulated that only 0.5 equiv of E is required in the reaction. Accordingly, we followed the reaction between 0.5 equiv of Se and complex **1** in py-d_5 by ^{1}H and ^{31}P NMR spectroscopy. The room temperature ^{1}H NMR spectrum of the

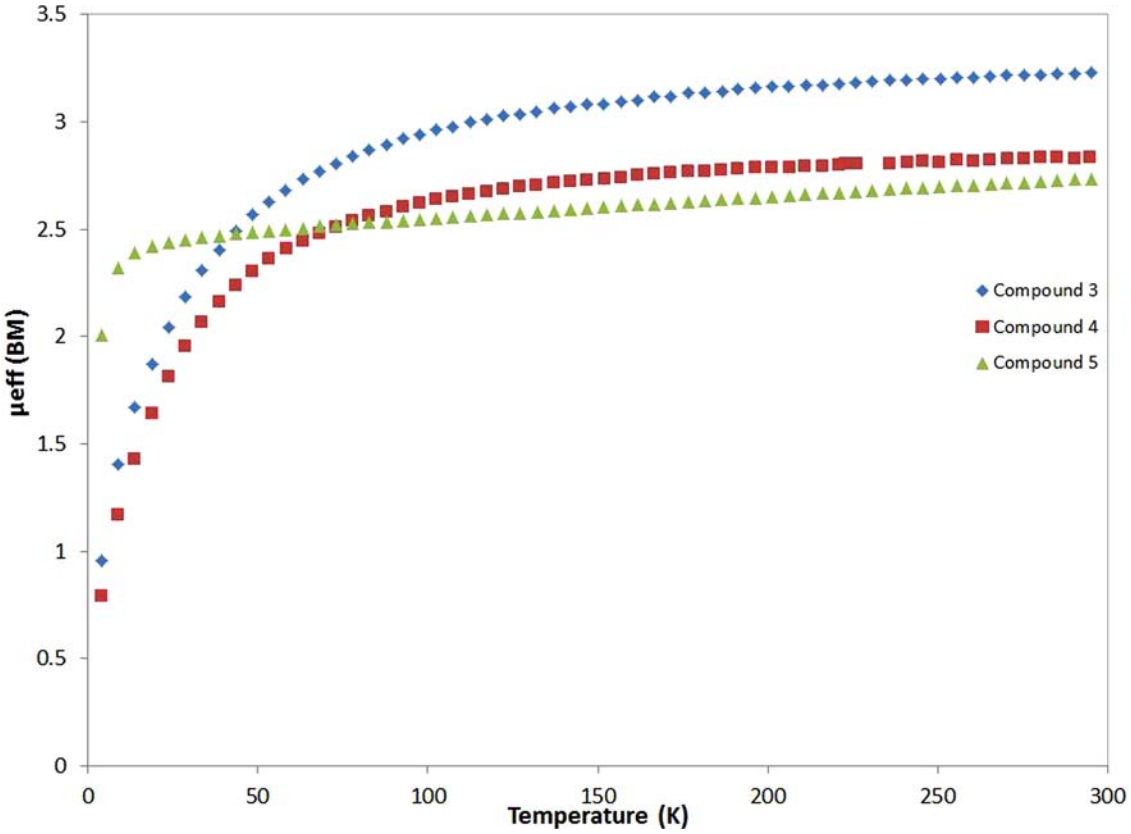

Figure 3. Temperature-dependent SQUID magnetization data for **3**–**5** from 4 to 300 K.

in situ reaction mixture reveals the formation of **3** and $U(CH_2SiMe_2NSiMe_3)(NR_2)_2$, in a 1.4:1 ratio,[50] in addition to the resonances of several unidentified minor products. Notably, all of complex **1** is consumed during the course of the reaction. In addition, at low temperature (−35 °C), the ^{31}P NMR spectrum of the reaction mixture features two resonances at 21.42 and 20.65 ppm, assignable to $[Ph_3PCH_3]^+$ and $Ph_3P{=}CH_2$, respectively. These are present in an approximately 2:1 ratio. Also present in the ^{31}P NMR spectrum is a small amount of Ph_3P, observed as a singlet at −6.46 ppm. On the basis of these observations, it is probable that only 0.5 equiv of E is required to achieve full conversion. Accordingly, the maximum yield for complexes **2**–**4** can only be 50% (based on uranium).

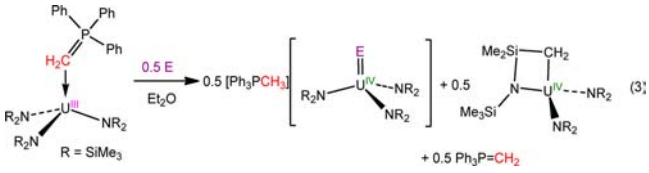

To account for the formation of **3** and $U(CH_2SiMe_2NSiMe_3)(NR_2)_2$, we suggest that addition of 0.5 equiv of Se to complex **1** produces 0.5 equiv of the putative "$U(Se)(NR_2)_3$" species, and leaves 0.5 equiv of unconsumed U(III) starting material. The U(III) starting material then acts as a H-atom source, resulting in formation of $U(SeH)(NR_2)_3$ and 1 equiv of $U(CH_2SiMe_2NSiMe_3)(NR_2)_2$ (eq 3). $U(SeH)(NR_2)_3$ is subsequently deprotonated by $Ph_3P{=}CH_2$ to give the final product, **3**. In support of this mechanism, we note that **3** can be isolated in similar yields regardless if 0.5 or 1 equiv of Se is used in the reaction. Additionally, both complex **1** and $U(NR_2)_3$ are known H· sources.[33,51,52] For example, complex **1** converts to $U(=CHPPh_3)(NR_2)_3$, $U(CH_3)(NR_2)_3$, and Ph_3P over the course of several hours in C_6D_6, via H· transfer between ylide ligands.[33,52] Similarly, the reaction between $U(NR_2)_3$ and the U(V) imido complex, $U(=NAr)(NR_2)_3$ (Ar = *p*-tolyl), yields the aforementioned U(IV) metallacycle, $U(CH_2SiMe_2NSiMe_3)(NR_2)_2$, and the U(IV) amide $U(NHAr)(NR_2)_3$, also via H· transfer.[51] Alternately, it is possible that the U(V) selenido metallacycle, $[Ph_3PCH_3][U(Se)(CH_2SiMe_2NSiMe_3)(N\{SiMe_3\}_2)_2]$, is initially generated. This material is then reduced by either **1** or $U(NR_2)_3$ to give the final products. Support for this pathway comes from the synthesis of its stable oxo analogue, $[Ph_3PCH_3][U(O)(CH_2SiMe_2NSiMe_3)(N\{SiMe_3\}_2)_2]$, which is formed by O-atom transfer to **1**.[33]

The use of $U(H_2C{=}PPh_3)(NR_2)_3$ as a precursor for the synthesis of the terminal chalcogenide ligands is also worthy of comment. We suggest that the ylide ligand in this material promotes the formation of the terminal chalcogenide by limiting the availability of $U(NR_2)_3$ in solution. This prevents formation of a bridging chalcogenide by slowing the rate of comproportionation between the putative terminal chalcogenide, $U(Se)(NR_2)_3$, and $U(NR_2)_3$.[18,24] The ylide may also play an important trapping role when it is protonated to produce $[Ph_3PCH_3]^+$.

To rule out other mechanistic pathways, we performed the synthesis of **3** in THF-d_8 on the preparative scale, specifically to determine whether H· abstraction involved the solvent. Under these conditions, complex **3** can be isolated in 25% yield; however, the isolated material exhibits no observable deuterium incorporation by ^2H NMR spectroscopy, suggesting that solvent is not the source of the proton found in the $[Ph_3PCH_3]^+$ cation. Additionally, we have performed the

dx.doi.org/10.1021/ja305712m | J. Am. Chem. Soc. 2012, 134, 15468–15475

synthesis of **3** in the presence of 9,10-dihydroanthrance. Under these conditions, the isolated yield of **3** is 16%, suggesting that the presence of 9,10-dihydroanthrance confers no advantage. We also followed the reaction of $U(D_2C{=}PPh_3)(NR_2)_3$ (R = $SiMe_3$) (**1-d_2**),[52] with 1 equiv of Se in py-d_5 by ^1H and ^{31}P NMR spectroscopy. However, this reaction is complicated by the scrambling of the ^2H label between the ylide methylene group and the $N(SiMe_3)_2$ ligands in **1-d_2** (see the Supporting Information). This scrambling, which we have observed previously,[52] occurs prior to its conversion into complex **3**. As a result, we observe ^2H incorporation into the $SiMe_3$ groups of complex **3**, along with ^1H incorporation into the methyl group of the phosphonium cation, negating our ability to conclusively demonstrate the origin of the extra proton in $[Ph_3PCH_3]^+$ by this method.

CONCLUSIONS

Addition of elemental chalcogens to the U(III) ylide adduct, $U(H_2C{=}PPh_3)(NR_2)_3$ (R = $SiMe_3$), results in the formation of the U(IV) terminal monochalcogenides, $[Ph_3PCH_3][U(E)(NR_2)_3]$ (E = S, Se, Te). X-ray structural characterization reveals short U−E bond lengths relative to U−E single bonds, suggestive of multiple bond character in the U−E interaction. During their formation, the ylide ligand in the starting material, $U(H_2C{=}PPh_3)(NR_2)_3$, likely promotes the formation of the terminal chalcogenide ligand by limiting the availability of $U(NR_2)_3$ in solution, thereby disfavoring the generation of the more common bridging chalcogenide ligand. This synthetic strategy may be broadly applicable to the generation of other actinide−chalcogenide multiple bonds. Additionally, this work further demonstrates that the U^{4+} ion is capable of supporting a diverse array of metal−ligand multiple bonds, and that the high oxidation state U^{5+} and U^{6+} ions are not necessarily required for the stabilization of multiply bonded ligands. For future work, we will probe the electronic structures of these complexes using both DFT calculations and X-ray absorption spectroscopy, specifically to address the extent of covalency in the U−E interaction, information that may be useful for the design of new soft donor extractants.

EXPERIMENTAL SECTION

General. All reactions and subsequent manipulations were performed under anaerobic and anhydrous conditions under an atmosphere of nitrogen or argon. Tetrahydrofuran (THF), hexanes, diethyl ether (Et_2O), and toluene were dried using a Vacuum Atmospheres DRI-SOLV Solvent Purification system and stored over 3 Å sieves for 24 h before use. Pyridine, pyridine-d_5, and C_6D_6 were dried over 3 Å molecular sieves for 24 h before use. Dimethoxyethane (DME) was distilled from sodium benzophenone ketyl and stored over 3 Å molecular sieves for 24 h before use. $U[N(SiMe_3)_2]_3$,[53] $[H_2CPPh_3][U[N(SiMe_3)_2]_3]$,[52] $[D_2CPPh_3][U[N(SiMe_3)_2]_3]$,[52] $U(O)[N(SiMe_3)_2]_3$,[39] $U(CH_2SiMe_2NR)[N(SiMe_3)_2]_3$ (R = $SiMe_3$),[54] Ph_3PCH_2,[55] Ph_3PCD_2,[52] and $[Ph_3PCH_3][PF_6]$[56] were synthesized according to the previously reported procedures. $NaN(SiMe_3)_2$ was recrystallized from toluene before use. Cp^*_2Co was recrystallized from hexanes before use. All other reagents were purchased from commercial suppliers and used as received.

NMR spectra were recorded on a Varian UNITY INOVA 400 or Varian UNITY INOVA 500 spectrometer. ^1H NMR spectra were referenced to external $SiMe_4$ using the residual protio solvent peaks as internal standards. $^{31}P\{^1H\}$ NMR spectra were referenced to external 85% H_3PO_4. IR spectra were recorded on a Nicolet 6700 FT-IR spectrometer with a NXR FT Raman Module. UV−vis/NIR experiments were performed on a UV-3600 Shimadzu spectrophotometer. Elemental analyses were performed by the Micro-Mass Facility at the University of California, Berkeley.

Magnetism Measurements. Magnetism data were recorded using a Quantum Design MPMS 5XL SQUID magnetometer. The experiments were performed between 4 and 300 K using 50−100 mg of powdered, crystalline solid. The solids were loaded into NMR tubes, which were subsequently flame-sealed. The solids were kept in place with approximately 100 mg of quartz wool packed on either side of the sample. The data were corrected for the contribution of the NMR tube holder and the quartz wool. The experiments were performed using a 0.5 T field. Diamagnetic corrections ($\chi_{dia} = -5.31 \times 10^{-4}$ cm^3 mol^{-1} for **3**; $\chi_{dia} = -5.45 \times 10^{-4}$ cm^3 mol^{-1} for **4**; $\chi_{dia} = -5.85 \times 10^{-4}$ cm^3 mol^{-1} for **5**) were made using Pascal's constants.

DOSY Spectroscopy. DOSY spectra were recorded at 25 °C on a Varian INOVA 600 spectrometer equipped with a cryoprobe, using a convection compensated DOSY scheme. Diffusion constants of the phosphonium salts reported here were normalized to the diffusion constant of the residual protio solvent (py-d_5) resonance at 8.74 ppm. For $[Ph_3PCH_3][I]$, the relative diffusion constant was determined to be 0.38, while for $[Ph_3PCH_3][PF_6]$, the relative diffusion constant was determined to be 0.40.

Synthesis of $[Ph_3PCH_3][U(S)[N(SiMe_3)_2]_3]$ (2). To a solution of $U(H_2C{=}PPh_3)[N(SiMe_3)_2]_3$ (248.4 mg, 0.250 mmol) in Et_2O (2 mL) was added elemental sulfur (9.0 mg, 0.281 mmol). A color change from deep purple to orange-red was observed within 2 min after addition. After 5 min, the solution was filtered through a Celite column (0.5 cm × 2 cm) supported on glass wool, and all volatiles were removed in vacuo. The resulting yellow solid was rinsed with Et_2O (3 mL), and then extracted into THF to give a yellow solution. The solution was concentrated to less than 1 mL and subsequently layered with hexanes (12 mL). Storage of this solution at −25 °C for 24 h resulted in the deposition of yellow powder (49.4 mg, 19% yield based on uranium). Crystals suitable for X-ray crystallography were grown from a py-d_5/C_6D_6 solution left at room temperature for several hours. ^1H NMR (400 MHz, 25 °C, py-d_5): δ −2.24 (br s, 54H, NSiMe_3), 1.43 (d, 3H, J_{PH} = 14 Hz, H_3CPPh_3), 7.05 (m, 6H, J_{HH} = 7 Hz, meta CH), 7.44 (br s, 6H, ortho CH), 7.72 (t, 3H, J_{HH} = 7 Hz, para CH). $^{31}P\{^1H\}$ NMR (162 MHz, 25 °C, py-d_5): δ 21.28 (br s). Anal. Calcd for $C_{37}H_{72}N_3SPSi_6U$: C, 43.22; H, 7.06; N, 4.09. Found: C, 43.58; H, 6.86; N, 3.89. UV−vis/NIR (OC_4H_8, 4.6 mM, 25 °C, L mol^{-1} cm^{-1}): 600 (ε = 25.3), 702 (ε = 41.9), 720 (ε = 36.9), 878 (ε = 7.7), 952 (ε = 8.6), 1124 (ε = 26.9), 1216 (ε = 34.1), 1392 (ε = 4.5), 1500 (ε = 9.1). IR (KBr pellet, cm^{-1}): 1589 (w), 1485 (w), 1439 (s), 1400 (w), 1344 (w), 1319 (w), 1248 (s), 1184 (m), 1167 (w), 1117 (s), 1074 (w), 1028 (w), 997 (m), 937 (s), 906 (m), 847 (s), 775 (s), 746 (s), 719 (m), 690 (s), 663 (s), 608 (s), 511 (m), 500 (m), 486 (m), 449 (w).

Synthesis of $[Ph_3PCH_3][U(Se)[N(SiMe_3)_2]_3]$ (3). To a solution of $U(H_2C{=}PPh_3)[N(SiMe_3)_2]_3$ (184.0 mg, 0.185 mmol) in Et_2O (2 mL) was added elemental selenium (15.4 mg, 0.195 mmol). A color change from deep purple to orange-red, concomitant with the deposition of a red-orange solid, was observed immediately upon addition. After 5 min, all volatiles were removed in vacuo, and the resulting crude reaction mixture was dissolved in THF (3 mL) and filtered through a Celite column (0.5 cm × 2 cm) supported on glass wool. The volume of the red-orange filtrate was reduced in vacuo to 0.5 mL, and the solution was subsequently layered with hexanes (12 mL). Storage of this solution at −25 °C for 24 h resulted in the deposition of red-orange powder (85.5 mg). Recrystallization from THF/hexanes yielded pure microcrystalline red-orange material (38.0 mg, 19% yield based on uranium). Red crystalline plates suitable for X-ray crystallography were grown from an Et_2O/hexanes solution left at room temperature for 2 h. ^1H NMR (400 MHz, 25 °C, py-d_5): δ −1.77 (br s, 54H, NSiMe_3), 1.57 (d, 3H, J_{PH} = 14 Hz, H_3CPPh_3), 6.83 (m, 6H, J_{HH} = 7.0 Hz, meta CH), 7.17 (m, 6H, J_{HH} = 3.8 Hz, ortho CH), 7.44 (t, 3H, J_{HH} = 7.0 Hz, para CH). $^{31}P\{^1H\}$ NMR (162 MHz, 25 °C, py-d_5): δ 20.10 (br s). DOSY NMR (600 MHz, 25 °C, py-d_5), relative diffusion constant of $[Ph_3PCH_3]^+$: 0.36. Anal. Calcd for $C_{37}H_{72}N_3SePSi_6U$: C, 41.36; H, 6.75; N, 3.91. Found: C, 41.65; H, 6.54; N, 3.57. UV−vis/NIR (OC_4H_8, 4.4 mM, 25 °C, L mol^{-1} cm^{-1}):

700 (ε = 36.3), 718 (ε = 36.8), 934 (ε = 11.5), 1122 (ε = 31.9), 1208 (ε = 34.6), 1512 (ε = 14.7), 1666 (ε = 15.7). IR (KBr pellet, cm^{-1}): 1589 (w), 1483 (w), 1439 (s), 1402 (w), 1344 (w), 1317 (w), 1248 (s), 1184 (w), 1165 (w), 1117 (m), 997 (w), 970 (m), 930 (s), 906 (s), 883 (m), 843 (s), 775 (s), 746 (s), 719 (m), 690 (s), 663 (s), 609 (s), 511 (m), 500 (m), 486 (m), 449 (w). Complex **3** exhibits an effective magnetic moment of 3.23 μ_B at 300 K, which decreases to 0.96 μ_B at 4 K.

Synthesis of $[Ph_3PCH_3][U(Se)[N(SiMe_3)_2]_3]$ (3) with 0.5 equiv of Se. To a solution of $U(H_2C{=}PPh_3)[N(SiMe_3)_2]_3$ (77.3 mg, 0.078 mmol) in Et_2O (2 mL) was added elemental selenium (3.3 mg, 0.042 mmol). A color change from deep purple to red-orange, concomitant with the deposition of a red-orange solid, was observed immediately upon addition. After 5 min, the supernatant was decanted off and discarded. The resulting solid was dried in vacuo, dissolved in THF (3 mL), and filtered through a Celite column (0.5 cm × 2 cm) supported on glass wool. The volume of the red-orange filtrate was reduced in vacuo to 0.5 mL, and the solution was layered with hexanes (15 mL). Storage of this solution at −25 °C for 24 h resulted in the deposition of red-orange powder (16.3 mg, 19% yield based on uranium). This material was spectroscopically identical to the material isolated upon reaction of **1** with 1 equiv of Se.

Synthesis of $[Ph_3PCH_3][U(Se)[N(SiMe_3)_2]_3]$ (3) in the Presence of 9,10-Dihydroanthracene. To a deep purple solution of $U(H_2C{=}PPh_3)[N(SiMe_3)_2]_3$ (301 mg, 0.304 mmol) in Et_2O (2 mL) was added 9,10-dihydroanthracene (20.0 mg, 0.111 mmol). No color change was observed upon addition. To this solution was added elemental selenium (42.0 mg, 0.532 mmol). A color change from deep purple to red-orange, concomitant with the deposition of a red-orange solid, was observed immediately upon addition. After 15 min, all volatiles were removed in vacuo, and the material was extracted into dimethoxyethane (4 mL) and filtered through a Celite column (0.5 cm × 2 cm) supported on glass wool. The volume of the red-orange filtrate was reduced in vacuo to 2 mL, and the solution was layered with hexanes (12 mL). Storage of this solution at −25 °C for 24 h resulted in the deposition of red-brown powder (53.2 mg, 16% yield based on uranium). This material was spectroscopically identical to the material isolated upon reaction of **1** with 0.5 or 1 equiv of Se.

Synthesis of $[Ph_3PCH_3][U(Te)[N(SiMe_3)_2]_3]$ (4). To a solution of $U(H_2C{=}PPh_3)[N(SiMe_3)_2]_3$ (316.2 mg, 0.318 mmol) in Et_2O (2 mL) was added elemental tellurium (40.7 mg, 0.319 mmol). A color change from deep purple to deep brown was observed within 5 min after addition. After 20 min, all volatiles were removed in vacuo to give a brown solid. The solid was extracted into DME (1 mL) and filtered through a Celite column (0.5 cm × 2 cm) supported on glass wool. The filtrate was subsequently layered with hexanes (12 mL). Storage of this solution at −25 °C for 24 h resulted in the deposition of brown powder (92.3 mg, 26% yield based on uranium). Crystals suitable for X-ray crystallography were grown from a dilute Et_2O (2 mL) solution left at room temperature for ∼6 h. ^1H NMR (400 MHz, 25 °C, py-d_5): δ −1.46 (br s, 54H, NSiMe_3), 1.63 (br s, 3H, H_3CPPh_3), 6.82 (br s, 6H, meta CH), 7.14 (br s, 6H, ortho CH), 7.41 (br s, 3H, para CH). $^{31}P\{^1H\}$ NMR (162 MHz, 25 °C, py-d_5): δ 20.14 (br s). Anal. Calcd for $C_{37}H_{72}N_3TePSi_6U$: C, 39.53; H, 6.46; N, 3.74. Found: C, 39.67; H, 6.35; N, 3.54. UV−vis/NIR (OC_4H_8, 3.8 mM, 25 °C, L mol^{-1} cm^{-1}): 952 (ε = 16.6), 1100 (ε = 27.9), 1196 (ε = 29.8), 1462 (ε = 10.8), 1564 (ε = 12.6), 1650 (ε = 15.8). IR (KBr pellet, cm^{-1}): 1587 (w), 1483 (w), 1438 (m), 1402 (w), 1344 (w), 1250 (s), 1184 (w), 1164 (w), 1115 (w), 968 (m), 916 (s), 883 (m), 845 (s), 773 (m), 746 (m), 719 (m), 690 (s), 662 (m), 609 (m), 509 (m), 501 (m), 486 (w), 451 (w). Complex **4** exhibits an effective magnetic moment of 2.83 μ_B at 300 K, which decreases to 0.79 μ_B at 4 K.

Synthesis of $[Cp^*_2Co][U(O)[N(SiMe_3)_2]_3]$ (5). To a solution of $U(O)[N(SiMe_3)_2]_3$ (403.8 mg, 0.550 mmol) in Et_2O (2 mL) was added Cp^*_2Co (179.7 mg, 0.546 mmol) dropwise as a Et_2O solution (8 mL). This resulted in the deposition of a tan precipitate. To this solution was added hexanes (12 mL), which caused further deposition of the tan solid. The solid was washed with hexanes (2 × 5 mL) and dried in vacuo. The solid was then extracted into THF (5 mL), and filtered through a Celite column (0.5 cm × 2 cm) supported on glass wool. The resulting solution was concentrated in vacuo and layered with hexanes (10 mL). Storage of this solution at −25 °C for 24 h resulted in the deposition of light brown crystals (474 mg, 81% yield). Crystals suitable for X-ray crystallography were grown by storage of a 1:1 toluene/THF solution at −25 °C for ∼2 h. ^1H NMR (400 MHz, 25 °C, py-d_5): δ −2.13 (br s, 54H, NSiMe_3), 3.40 (s, 30H, Cp^*_2Co). Anal. Calcd for $C_{38}H_{84}N_3OSi_6CoU$: C, 42.87; H, 7.95; N, 3.95. Found: C, 42.66; H, 7.51; N, 3.80. UV−vis/NIR (OC_4H_8, 5.0 mM, 25 °C, L mol^{-1} cm^{-1}): 532 (ε = 73.6), 606 (ε = 26.5), 704 (ε = 44.6), 842 (ε = 15.7), 904 (ε = 21.6), 968 (ε = 5.5), 1078 (ε = 9.9), 1178 (ε = 14.5), 1426 (ε = 36.6), 1544 (ε = 30.7). IR (KBr pellet, cm^{-1}): 1477 (w), 1454 (w), 1427 (s), 1387 (w), 1379 (w), 1248 (s), 1238 (s), 1184 (w), 1080 (w), 1024 (m), 993 (s), 937 (m), 879 (m), 864 (s), 841 (s), 831 (s), 766 (m), 756 (m), 687 (w), 663 (m), 598 (m). Complex **5** exhibits an effective magnetic moment of 2.73 μ_B at 300 K, which decreases to 2.00 μ_B at 4 K.

Synthesis of $[Ph_3PCH_3][U(Se)[N(SiMe_3)_2]_3]$ (3) with 1 equiv of Se in THF-d_8. To a solution of $U(H_2C{=}PPh_3)[N(SiMe_3)_2]_3$ (95.6 mg, 0.096 mmol) in THF-d_8 (2 mL) was added elemental selenium (8.0 mg, 0.10 mmol). A color change from deep purple to red-orange was observed immediately upon addition. After 5 min, the solution filtered through a Celite column (0.5 cm × 2 cm) supported on glass wool to give a red-orange filtrate. The filtrate was concentrated in vacuo to 0.5 mL and subsequently layered with hexanes (15 mL). Storage of this solution at −25 °C for 24 h resulted in the deposition of red-orange powder (24.7 mg, 25% yield based on uranium). This material was spectroscopically identical to the material isolated upon reaction of **1** with 1 equiv of Se in Et_2O. ^1H NMR (400 MHz, 25 °C, py-d_5): δ −1.76 (br s, 54H, NSiMe_3), 1.05 (d, 3H, J_{PH} = 14 Hz, H_3CPPh_3), 6.57 (m, 6H, J_{HH} = 7.1 Hz, meta CH), 6.99 (s, 6H, ortho CH), 7.31 (s, 3H, para CH). $^{31}P\{^1H\}$ NMR (162 MHz, 25 °C, py-d_5): δ 19.76 (s). In the ^2H NMR spectrum, only signals attributable to THF-d_8 and py-d_5 were observed. No resonances indicative of deuterium incorporation into the product were observed.

In Situ Synthesis of $[Ph_3PCH_3][U(Se)[N(SiMe_3)_2]_3]$ (3) with 1 equiv of Se in py-d_5. An NMR tube was charged with a solution of **1** (14.1 mg, 0.014 mmol) in py-d_5 (0.5 mL), whereupon Se (1.0 mg, 0.013 mmol) was added. Upon addition, the deep blue-purple solution immediately turned orange in color. Both complex **3** and $U(CH_2SiMe_2NR)(NR_2)_2$ were observed in solution, in addition to several unidentified products. ^1H NMR (400 MHz, 25 °C, py-d_5): δ −7.32 (s, 36H, NSiMe_3, $U(CH_2SiMe_2NR)(NR_2)_2$), −1.75 (s, 54H, NSiMe_3, **3**), 1.48 (s, 3H, H_3CPPh_3, **3**), 6.75 (br s, 6H, meta CH, **3**), 7.05 (br s, 6H, ortho CH, **3**), 7.38 (t, 3H, para CH, **3**), 16.38 (s, 6H, $CH_2SiMe_2NSiMe_3$, $U(CH_2SiMe_2NR)(NR_2)_2$), 19.67 (s, 9H, $CH_2SiMe_2NSiMe_3$, $U(CH_2SiMe_2NR)(NR_2)_2$). $^{31}P\{^1H\}$ NMR (162 MHz, 25 °C, py-d_5): δ 19.77 (s).

In Situ Synthesis of $[Ph_3PCH_3][U(Se)[N(SiMe_3)_2]_3]$ (3) with 0.5 equiv of Se in py-d_5. An NMR tube was charged with a solution of **1** (40.0 mg, 0.040 mmol) in py-d_5 (0.5 mL), whereupon Se (1.6 mg, 0.020 mmol) was added. Upon addition, the deep blue-purple solution immediately turned deep red-orange in color. Both complex **3** and $U(CH_2SiMe_2NR)(NR_2)_2$ were observed in the sample, in addition to several unidentified products. ^1H NMR (400 MHz, 25 °C, py-d_5): δ −7.25 (s, 36H, NSiMe_3, $U(CH_2SiMe_2NR)(NR_2)_2$), −1.66 (s, 54H, NSiMe_3, **3**), 0.79 (s, 3H, H_3CPPh_3, **3**), 6.39 (br s, 6H, meta CH, **3**), 6.87 (br s, 6H, ortho CH, **3**), 7.46 (t, 3H, para CH, **3**), 16.75 (s, 6H, $CH_2SiMe_2NSiMe_3$, $U(CH_2SiMe_2NR)(NR_2)_2$), 20.16 (s, 9H, $CH_2SiMe_2NSiMe_3$, $U(CH_2SiMe_2NR)(NR_2)_2$). $^{31}P\{^1H\}$ NMR (162 MHz, 25 °C, py-d_5): δ 21.01 (s).

Reaction of $[U(D_2CPPh_3)[N(SiMe_3)_2]_3]$ with 1 equiv of Se in py-d_5. A J-Young NMR tube was charged with a solution of **1**-d_2 (23.4 mg, 0.023 mmol) in py-d_5 (0.5 mL), whereupon Se (2.3 mg, 0.029 mmol) was added. Upon addition, the deep blue-purple solution immediately turned red-orange in color. Complex **3** was observed in the sample, in addition to several unidentified products. ^1H NMR (400 MHz, 25 °C, py-d_5): δ −1.73 (s, 54H, NSiMe_3, **3**), 1.17 (br s, 3H, H_3CPPh_3, **3**), 6.44 (br s, 6H, meta CH, **3**), 6.83 (br s, 6H, ortho CH, **3**), 7.13 (t, 3H, para CH, **3**). $^{31}P\{^1H\}$ NMR (162 MHz, 25 °C, py-d_5):

Table 2. X-ray Crystallographic Data for Complexes 5, 2, 3, and 4

	5	2	3	4
empirical formula	$UOC_{38}H_{84}N_3Si_6Co$	$UC_{37}H_{72}N_3Si_6PS$	$UC_{37}H_{72}N_3Si_6PSe$	$UC_{37}H_{72}N_3Si_6PTe$
crystal habit, color	plates, colorless	block, yellow	plates, red	plates, red-brown
crystal size (mm)	0.25 × 0.25 × 0.15	0.2 × 0.2 × 0.2	0.05 × 0.4 × 0.4	0.05 × 0.4 × 0.4
crystal system	monoclinic	monoclinic	monoclinic	monoclinic
space group	$P2_1/n$	$P2_1/c$	$P2_1/c$	$P2_1/c$
volume (Å^3)	5153.7(6)	4888.8(2)	4905.4(2)	4974(2)
a (Å)	19.8951(15)	16.9301(4)	16.9733(4)	17.1540(4)
b (Å)	14.0270(10)	12.0740(4)	12.0775(4)	12.0776(3)
c (Å)	20.5125(13)	24.2248(7)	24.2638(7)	24.4001(6)
α (deg)	90.00	90.00	90.00	90.00
β (deg)	115.802(4)	99.155(2)	99.525(2)	100.3100(10)
γ (deg)	90.00	90.00	90.00	90.00
Z	4	4	4	4
formula weight (g/mol)	1064.58	1028.58	1075.48	1124.12
density (calculated) (Mg/m^3)	1.372	1.397	1.456	1.501
absorption coefficient (mm^{-1})	3.629	3.570	4.257	4.042
F_{000}	2176	2088	2160	2232
total no. reflections	30 687	64 654	22 147	63 797
unique reflections	10 537	24 144	10 698	29 492
R_{int}	0.0457	0.0457	0.0405	0.0364
final R indices [$I > 2\sigma(I)$]	R_1 = 0.0461, wR_2 = 0.0917	R_1 = 0.0342, wR_2 = 0.0634	R_1 = 0.0555, wR_2 = 0.1334	R_1 = 0.0354, wR_2 = 0.0712
largest diff. peak and hole (e Å^{-3})	4.119 and −2.828	2.661 and −1.920	8.549 and −5.217	3.741 and −2.850
GOF	1.115	0.994	1.339	1.001

δ 19.55 (s). ^{2}H NMR (77 MHz, 25 °C, py-d_5): δ 0.98 (s, H_3CPPh_3), −1.73 (s, NSiMe_3, **3**).

Monitoring the Formation of $[Ph_3PCH_3][U(Se)(NR_2)_3]$ (R = $SiMe_3$) via ^{31}P NMR Spectroscopy. To a vial charged with 19.7 mg (0.020 mmol) of complex **1** in py-d_5 (0.5 mL) was added 1.0 mg (0.013 mmol) of Se. A color change from deep blue-purple to orange was observed immediately. The solution was then transferred to an NMR tube equipped with a J-Young valve and monitored by variable-temperature ^{31}P{^{1}H} NMR spectroscopy. ^{31}P{^{1}H} NMR (162 MHz, 25 °C, py-d_5): δ 21.18 (s). ^{31}P{^{1}H} NMR (162 MHz, −35 °C, py-d_5): δ 21.42 (s, $[Ph_3PCH_3]^+$), 20.65 (s, $H_2C{=}PPh_3$).

X-ray Crystallography. Data for **2**, **3**, **4**, and **5** were collected on a Bruker KAPPA APEX II diffractometer equipped with an APEX II CCD detector using a TRIUMPH monochromator with a Mo Kα X-ray source (α = 0.71073 Å). The crystals of **2**, **3**, **4**, and **5** were mounted on a cryoloop under Paratone-N oil, and all data were collected at 100(2) K using an Oxford nitrogen gas cryostream system. Frame exposures of 10 s were used for **3**, **4**, and **5**. Frame exposures of 15 s were used for **2**. Data collection and cell parameter determination were conducted using the SMART program.[57] Integration of the data frames and final cell parameter refinement were performed using SAINT software.[58] Absorption correction of the data for **2**, **3**, **4**, and **5** was carried out using the multiscan method SADABS.[59] Subsequent calculations were carried out using SHELXTL.[60] Structure determination was done using direct or Patterson methods and difference Fourier techniques. All hydrogen atom positions were idealized and rode on the atom of attachment with exceptions noted in the subsequent paragraph. Structure solution, refinement, graphics, and creation of publication materials were performed using SHELXTL.[60]

A summary of relevant crystallographic data for complexes **2**, **3**, **4** and **5** is presented in Table 2.

■ ASSOCIATED CONTENT

Supporting Information

Crystallographic details (as CIF files) and spectral data for **2**−**5**. This material is available free of charge via the Internet at http://pubs.acs.org.

■ AUTHOR INFORMATION

Corresponding Author

hayton@chem.ucsb.edu

Notes

The authors declare no competing financial interest.

■ ACKNOWLEDGMENTS

This work was supported by the U.S. Department of Energy, Office of Basic Energy Sciences, Chemical Sciences, Biosciences, and Geosciences Division under Contract No. DE-FG02-09ER16067. The research carried out here made use of the SQUID magnetometer of the Materials Research Laboratory: an NSF MRSEC, supported by NSF DMR 1121053. The MRL is a member of the NSF-supported Materials Research Facilities Network. We also thank Hongjun Zhou for assistance with the DOSY spectroscopy measurements.

■ REFERENCES

(1) Ingram, K. I. M.; Kaltsoyannis, N.; Gaunt, A. J.; Neu, M. P. *J. Alloys Compd.* **2007**, *444*−*445*, 369−375.

(2) Madic, C.; Lecomte, M.; Baron, P.; Boullis, B. *C. R. Phys.* **2002**, *3*, 797−811.

(3) Mehdoui, T.; Berthet, J.-C.; Thuery, P.; Ephritikhine, M. *Chem. Commun.* **2005**, 2860−2862.

(4) Jensen, M. P.; Bond, A. H. *J. Am. Chem. Soc.* **2002**, *124*, 9870−9877.

(5) Miguirditchian, M.; Guillaneux, D.; Guillaumont, D.; Moisy, P.; Madic, C.; Jensen, M. P.; Nash, K. L. *Inorg. Chem.* **2005**, *44*, 1404−1412.

(6) Ingram, K. I. M.; Tassell, M. J.; Gaunt, A. J.; Kaltsoyannis, N. *Inorg. Chem.* **2008**, *47*, 7824−7833.

(7) Gaunt, A. J.; Reilly, S. D.; Enriquez, A. E.; Scott, B. L.; Ibers, J. A.; Sekar, P.; Ingram, K. I. M.; Kaltsoyannis, N.; Neu, M. P. *Inorg. Chem.* **2007**, *47*, 29−41.

(8) Cantat, T.; Graves, C. R.; Scott, B. L.; Kiplinger, J. L. *Angew. Chem., Int. Ed.* **2009**, *48*, 3681.

(9) Lam, O. P.; Heinemann, F. W.; Meyer, K. *Chem. Sci.* **2011**, *2*, 1538−1547.
(10) Brennan, J. G.; Andersen, R. A.; Zalkin, A. *Inorg. Chem.* **1986**, *25*, 1761−1765.
(11) Gaunt, A. J.; Scott, B. L.; Neu, M. P. *Inorg. Chem.* **2006**, *45*, 7401−7407.
(12) Avens, L. R.; Barnhart, D. M.; Burns, C. J.; McKee, S. D.; Smith, W. H. *Inorg. Chem.* **1994**, *33*, 4245−4254.
(13) Leverd, P. C.; Arliguie, T.; Ephritikhine, M.; Nierlich, M.; Lance, M.; Vigner, J. *New J. Chem.* **1993**, *17*, 769−771.
(14) Evans, W. J.; Montalvo, E.; Ziller, J. W.; DiPasquale, A. G.; Rheingold, A. L. *Inorg. Chem.* **2010**, *49*, 222−228.
(15) Ren, W.; Zi, G.; Fang, D.-C.; Walter, M. D. *J. Am. Chem. Soc.* **2011**, *133*, 13183−13196.
(16) Spencer, L. P.; Yang, P.; Scott, B. L.; Batista, E. R.; Boncella, J. M. *Inorg. Chem.* **2009**, *48*, 11615−11623.
(17) Lam, O. P.; Castro, L.; Kosog, B.; Heinemann, F. W.; Maron, L.; Meyer, K. *Inorg. Chem.* **2012**, *51*, 781−783.
(18) Hayton, T. W. *Dalton Trans.* **2010**, *39*, 1145−1158.
(19) Evans, W. J.; Kozimor, S. A.; Ziller, J. W. *Polyhedron* **2004**, *23*, 2689−2694.
(20) Williams, V. C.; Muller, M.; Leech, M. A.; Denning, R. G.; Green, M. L. H. *Inorg. Chem.* **2000**, *39*, 2538−2541.
(21) Brown, D. R.; Denning, R. G. *Inorg. Chem.* **1996**, *35*, 6158−6163.
(22) Bart, S. C.; Anthon, C.; Heinemann, F. W.; Bill, E.; Edelstein, N. M.; Meyer, K. *J. Am. Chem. Soc.* **2008**, *130*, 12536−12546.
(23) Kosog, B.; La Pierre, H. S.; Heinemann, F. W.; Liddle, S. T.; Meyer, K. *J. Am. Chem. Soc.* **2012**, *134*, 5284−5289.
(24) Roussel, P.; Boaretto, R.; Kingsley, A. J.; Alcock, N. W.; Scott, P. *J. Chem. Soc., Dalton Trans.* **2002**, 1423−1428.
(25) Arney, D. S. J.; Burns, C. J.; Smith, D. C. *J. Am. Chem. Soc.* **1992**, *114*, 10068−10069.
(26) Arney, D. S. J.; Burns, C. J. *J. Am. Chem. Soc.* **1993**, *115*, 9840−9841.
(27) Arney, D. S. J.; Burns, C. J. *J. Am. Chem. Soc.* **1995**, *117*, 9448−9460.
(28) Mills, D. P.; Cooper, O. J.; Tuna, F.; McInnes, E. J. L.; Davies, E. S.; McMaster, J.; Moro, F.; Lewis, W.; Blake, A. J.; Liddle, S. T. *J. Am. Chem. Soc.* **2012**, *134*, 10047−10054.
(29) Kraft, S. J.; Walensky, J.; Fanwick, P. E.; Hall, M. B.; Bart, S. C. *Inorg. Chem.* **2010**, *49*, 7620−7622.
(30) Zi, G.; Jia, L.; Werkema, E. L.; Walter, M. D.; Gottfriedsen, J. P.; Andersen, R. A. *Organometallics* **2005**, *24*, 4251−4264.
(31) Gong, Y.; Wang, X.; Andrews, L.; Schlader, T.; Riedel, S. *Inorg. Chem.* **2012**, *51*, 6983−6991.
(32) Ventelon, L.; Lescop, C.; Arliguie, T.; Leverd, P.; Lance, M.; Nierlich, M.; Ephritikhine, M. *Chem. Commun.* **1999**, 659−660.
(33) Fortier, S.; Kaltsoyannis, N.; Wu, G.; Hayton, T. W. *J. Am. Chem. Soc.* **2011**, *133*, 14224−14227.
(34) Leverd, P. C.; Lance, M.; Vigner, J.; Nierlich, M.; Ephritikhine, M. *J. Chem. Soc., Dalton Trans.* **1995**, 237−244.
(35) Liang, B.; Andrews, L.; Ismail, N.; Marsden, C. J. *Inorg. Chem.* **2002**, *41*, 2811−2813.
(36) Kuchta, M. C.; Parkin, G. *Chem. Commun.* **1994**, 1351−1352.
(37) Steiner, T. *J. Mol. Struct.* **1998**, *447*, 39−42.
(38) Cordero, B.; Gomez, V.; Platero-Prats, A. E.; Reves, M.; Echeverria, J.; Cremades, E.; Barragan, F.; Alvarez, S. *Dalton Trans.* **2008**, 2832−2838.
(39) Fortier, S.; Brown, J. L.; Kaltsoyannis, N.; Wu, G.; Hayton, T. W. *Inorg. Chem.* **2012**, *51*, 1625−1633.
(40) Reynolds, J. G.; Zalkin, A.; Templeton, D. H.; Edelstein, N. M. *Inorg. Chem.* **1977**, *16*, 1090−1096.
(41) Schelter, E. J.; Yang, P.; Scott, B. L.; Thompson, J. D.; Martin, R. L.; Hay, P. J.; Morris, D. E.; Kiplinger, J. L. *Inorg. Chem.* **2007**, *46*, 7477−7488.
(42) Castro-Rodriguez, I.; Meyer, K. *Chem. Commun.* **2006**, 1353−1368.
(43) Bart, S. C.; Heinemann, F. W.; Anthon, C.; Hauser, C.; Meyer, K. *Inorg. Chem.* **2009**, *48*, 9419−9426.
(44) Lam, O. P.; Bart, S. C.; Kameo, H.; Heinemann, F. W.; Meyer, K. *Chem. Commun.* **2010**, *46*, 3137−3139.
(45) Lam, O. P.; Anthon, C.; Heinemann, F. W.; O'Connor, J. M.; Meyer, K. *J. Am. Chem. Soc.* **2008**, *130*, 6567−6576.
(46) Lam, O. P.; Feng, P. L.; Heinemann, F. W.; O'Connor, J. M.; Meyer, K. *J. Am. Chem. Soc.* **2008**, *130*, 2806−2816.
(47) Kozimor, S. A.; Bartlett, B. M.; Rinehart, J. D.; Long, J. R. *J. Am. Chem. Soc.* **2007**, *129*, 10672−10674.
(48) Fortier, S.; Melot, B. C.; Wu, G.; Hayton, T. W. *J. Am. Chem. Soc.* **2009**, *131*, 15512−15521.
(49) Wang, X.; Andrews, L.; Marsden, C. J. *Inorg. Chem.* **2009**, *48*, 6888−6895.
(50) Simpson, S. J.; Turner, H. W.; Andersen, R. A. *Inorg. Chem.* **1981**, *20*, 2991−2995.
(51) Stewart, J. L. Tris[bis(trimethylsilyl)amido]uranium: Compounds with Tri-, Tetra-, and Penta-valent Uranium. Ph.D. Thesis, University of California, Berkeley, Berkeley, CA, 1988.
(52) Fortier, S.; Walensky, J. R.; Wu, G.; Hayton, T. W. *J. Am. Chem. Soc.* **2011**, *133*, 6894−6897.
(53) Andersen, R. A. *Inorg. Chem.* **1979**, *18*, 1507−1509.
(54) Simpson, S. J.; Andersen, R. A. *J. Am. Chem. Soc.* **1981**, *103*, 4063−4066.
(55) Bestmann, H. J.; Stransky, W.; Vostrowsky, O. *Chem. Ber.* **1976**, *109*, 1694−1700.
(56) Moreno, A.; Pregosin, P. S.; Veiros, L. F.; Albinati, A.; Rizzato, S. *Chem.-Eur. J.* **2008**, *14*, 5617−5629.
(57) *SMART Apex II*, Version 2.1; Bruker AXS Inc.: Madison, WI, 2005.
(58) *SAINT Software User's Guide*, Version 7.34a; Bruker AXS Inc.: Madison, WI, 2005.
(59) Sheldrick, G. M. *SADABS*; University of Gottingen: Germany, 2005.
(60) *SHELXTL PC*, Version 6.12; Bruker AXS Inc.: Madison, WI, 2005.